HHS Public Access

Author manuscript

Chaos Solitons Fractals. Author manuscript; available in PMC 2022 June 27.

Published in final edited form as:

Chaos Solitons Fractals. 2021 December ; 153(Pt 1): . doi:10.1016/j.chaos.2021.111419.

Control and Anticontrol of chaos in Fractional-order models of Diabetes, HIV, Dengue, Migraine, Parkinson's and Ebola Virus diseases

Manashita Borah[1,a*], **Debanita Das**[1], **Antara Gayan**[1], **Flavio Fenton**[2,b], **Elizabeth Cherry**[3,c]

[1]Department of Electrical Engineering, Tezpur University, Assam, 784028, India

[2]School of Physics, Georgia Institute of Technology, Atlanta, USA

[3]School of Computational Science and Engineering, Georgia Institute of Technology, Atlanta, USA

Abstract

This work proposes new fractional-order (FO) models of six chaotic diseases whose fractional dynamics have not been studied so far in literature. Secondly, design and analysis of suitable controllers to control chaos where present, and that of anticontrollers to generate chaos where absent, for these newly proposed FO models of diseases, are put forward. The proposed controllers and anticontrollers address the problem of the health hazards arising from the dysfunctionalities due to the impact of chaos in these biological models. Controllers to supress chaos in four diseases, namely, FO Diabetes Mellitus, FO Human Immunodeficiency Virus (HIV), FO Ebola Virus and FO Dengue models are designed by Back-stepping, Adaptive Feedback and Sliding Mode Control strategies, whereas anticontrollers to introduce chaos in diseases, namely, FO Parkinson's illness and FO Migraine models, are carried out by Linear State Feedback, Single State Sinusoidal Feedback and Sliding Mode Anticontrol strategies. The equilibrium points, eigenvalues and Lyapunov Exponents of the FO disease models are evaluated and indicate the significance of chaos in them and necessitate upon the requirement of controllers and anticontrollers accordingly. The simulation results in terms of bifurcation diagrams, time series plots and phase portraits confirm the successful accomplishment of the control objectives.

Keywords

chaos; controller; anticontroller; biological models; diseases; fractional order

1. Introduction

Chaos, a nonlinear phenomenon found in numerous physical systems, is deterministic in nature and displays the characteristics of sensitivity to initial conditions (SIC), aperiodicity [1], and unstable periodic orbits [N1]. It is the behaviour and governing mechanism of

[a*] manabor@tezu.ernet.in . [b] ffenton@gatech.edu . [c] elizabeth.cherry@gatech.edu .

dynamical systems that are characterized by disordered surfaces with underlying order and indicated by a positive maximum Lyapunov Exponent (MLE) [2].

Fractional calculus is almost as old as calculus having originated with Leibniz, and it has been applied to modelling biological circuits such as electrical wave propagation in human tissue [N1] and plant physiology. Fractional derivatives in time introduce memory into the system, as the dynamics depend on prior states with appropriate weighting, and can further complicate the behavior of chaotic systems.

It has been established that some amount of chaos is generally present in biological systems [3] including the complex network of the neuronal connectivity in the brain and the electrical activity of the human heart, but the prevalence and impact of chaotic dynamics on the operation of vital organs continues to be studied. For example, the importance of chaos in the field of biology and medicine, the adaptation of definite disease control methods and the behavioural aspects of disease complexities have been explained epidemiologically in [4]. In particular, determination of the nature of outbreaks of epidemics helps elucidate their courses of action and, thereby, provides insights into the formulation of control measures to curb their dissemination, reduce symptoms of the diseases, and identify efficient strategies for cure and prevention. Research on the development of models of diseases to understand their dynamics and progression is garnering attention with the outbreak and transmission of new diseases. Table 1 presents a brief review of papers of recent years on chaotic diseases, their types of model and control measures developed, if any.

Control and anticontrol of chaos in biological systems [33] have received much attention and typically involves inhibition of chaotic motions and attainment of stabilization towards an equilibrium point by conversion of a chaotic trajectory into a non-chaotic one. For instance, control of chaos in a glucose-insulin regulatory (GIR) model [14] may help to prevent diseases such as Type 1 Diabetes, Type 2 Diabetes, hypoglycaemia, hyperinsulinemia, etc. In 2016, an integer-order (IO) model of Ebola Virus Disease (EVD) that broke out in West Africa, formulated from data gathered by the World Health Organization, is characterised by chaotic dynamics whose unpredictable nature made the development of an early alert system and prior preparation for the epidemic challenging [25]. In fact, without control measures, EVD would have spread with a rate of 9300 deaths per year. On the other hand, biological systems may also call for anticontrol measures to generate chaos to ensure healthy functioning. For instance, in biophysical models of the electrical activity of the human brain, the state of a disease is characterized by an absence of chaotic behaviour [34], which may lead to Alzheimer’s disease, epilepsy [7], Migraine [15], Parkinson’s illness (PI) [23] and other such neurological disorders. This absence of chaos justifies the requirement of anticontrollers to introduce chaos in these diseases to curb their development. Recently, a number of methods to control chaos in various physical systems have been reported, such as Sliding Mode Control (SMC) [35], Back-stepping Control (BSC) [36], Active Control Method (ACM) [37], Adaptive Feedback Control (AFC) [38], and microcontroller synchronisation [39]. Similarly, anticontrol methods to introduce chaos in a particular disease/biological model may be performed by Linear State Feedback Anticontrol (LSFAC) [40], Single State Sinusoidal Feedback Anticontrol (SSSFAC) [41] and Sliding Mode Anticontrol (SMAC).

In general, these controllers and anticontrollers have been minimally used for fractional-order disease models despite the importance of fractional-order models in this context. It is noteworthy in Table 1 that recent models of diseases such as Diabetes Mellitus [14], HIV infection [22], EVD [25], Dengue [4], Migraine [15] and Parkinson's illness [23] have been confined only to IO models and without any report on design of controllers. Such IO models lack the information of memory and learning mechanism present in fractional-order (FO) models. Second, FO models give a deeper understanding of complex behaviour that may remain unobserved in the IO models. Third, fractional dynamics in many cases provides a closer fit to the biophysical system than IO models [1,2,42]. The six diseases mentioned are typically modelled using IO approaches and also lack the solutions to deal with the impact of chaos in disease propagation. This is an open problem at large and our paper attempts to tackle it by presenting methods that will control the spread of the diseases [14,22,25,4,15,23] when fractional dynamics are incorporated.

Here, we analyse the existence of chaos in fractional dynamics of some recent disease models and propose the design of new and suitable control and anticontrol methods to eliminate and induce chaos, respectively, so as to impede progression of the disease state. This work is done with a view to eliminating the limitations mentioned and to aid in adopting precautionary measures to avoid progression of the diseases. Chaos suppression is referred to as 'control of chaos' and chaos generation is referred to as 'anticontrol of chaos' throughout this paper. The novelty of this work is highlighted as follows:

- **i.** Proposal of fractional-order models of six diseases and analysing the impact of chaos in them.
- **ii.** Design of appropriate controllers to stabilise chaos in diseases where chaos is undesirable.
- **iii.** Design of appropriate anticontrollers to generate chaos in diseases where chaos is essential.

The rest of this paper is organised as follows. Section 2 provides the FO models of the six diseases and their analyses. Section 3 presents the design of controllers and anticontrollers and is followed by a discussion of the results in Section 4. The paper is concluded in Section 5.

2. Fractional-order disease models, their computation and analyses

The FO preliminaries used in this paper are given below.

2.1 Preliminaries of FO

The Caputo fractional derivative of order α of a continuous function $f(t)$ is defined in (1).

$$D_t^{\alpha} f(t) = \frac{d^{\alpha} f(t)}{dt^{\alpha}} =$$

$$\begin{cases} \frac{1}{\Gamma(w-\alpha)} \int_0^t \frac{f^{(w)}(\tau)}{(t-\tau)^{\alpha - w + 1}} d\tau, & w - 1 < \alpha < w, \quad w \in N \\ \frac{d^w}{dt^w} f(t), & \alpha = w \end{cases} \tag{1}$$

Let us define an FO nonlinear system (FONLS) as in (2):

$$D_t^{\alpha} x_i(t) = f_i(X(t), t), \tag{2}$$

where the FOs lie in $0 < \alpha < 1$ and $X(t) = [x_1, x_2, \ldots, x_n]^T$, $(i = 1, 2, \ldots, n)$.

Theorem 1: The equilibrium points of a commensurate FONLS are asymptotically stable if for all the eigenvalues $\lambda_i (i = 1, 2, \ldots, n)$ of the Jacobian matrix $J = {}^{\partial f}/_{\partial x}$, where $f = [f_1, f_2, \ldots f_n]^T$, evaluated at the equilibrium point satisfy the condition $|arg(eig(J))| = |arg(\lambda_i)| > \alpha\pi/2$, $i = 1,2, \ldots, n$.

Lemma 1: [43] If $x(t) \in \mathbb{R}$ is a continuous and derivable function, then, for any time $t \geq 0$,

$$\frac{1}{2} D^{\alpha} x^2(t) \leq x(t) D^{\alpha} x(t), \qquad \forall \alpha \in (0, 1]$$

where $D^{\alpha} x(t)$ is the Caputo fractional derivative of $x(t)$ of FO α.

2.2 Computation of the fractional-order differential equations (FODEs)

The Adams-Bashforth-Moulton (ABM) method based on the predictor-corrector technique [44] is used to solve the FODEs numerically. The FONLS (2) may be written in a Volterra integral equation as,

$$x_i(t) = x_i(0) + \frac{1}{\Gamma\alpha} \int_0^t (t-\tau)^{\alpha - 1} f_i(x_1, x_2, \ldots, x_n) d\tau, \tag{3}$$

where $x_i(0)$ are the initial conditions (ICs) of $x_i(t)$.

The corrector equation obtained by substituting $h = \frac{T}{N}$, $t_n = nh$, for $(n = 0,1, \ldots, N)$ for a unique solution in $[0, T]$ is as in (4).

$$x_{ih}(t_{n+1}) = x_i(0) + \frac{h^{\alpha}}{\Gamma(\alpha+2)} f_i\left(x_{1h}^p(t_{n+1}), x_{2h}^p(t_{n+1}), \ldots, x_{nh}^p(t_{n+1})\right) + \frac{h^{\alpha}}{\Gamma(\alpha+2)} \sum a_{i,j,n+1} f_i\left(x_1(t_j), x_2(t_j), \ldots, x_n(t_j)\right) \tag{4}$$

where

$$a_{i,j,n+1} = \begin{cases} n^{\alpha+1} - (n-\alpha)(n+1)^{\alpha}, & if\ j = 0 \\ (n-j+2)^{\alpha+1} + (n-j)^{\alpha+1} - 2(n-j+1)^{\alpha+1}, & if\ 1 \le j \le n \\ 1, & if\ j = n+1 \end{cases}$$

The predicted value $x_{ih}^{p}(t_{n+1})$ is determined by

$$x_{ih}^{p}(t_{n+1}) = x_i(0) + \frac{1}{\Gamma(\alpha)} \sum_{j=0}^{n} b_{i,j,n+1} f_i\left(x_{ih}(t_j)\right), \tag{5}$$

where $b_{i,j,n+1} = \frac{h^{\alpha}}{\alpha}\left((n-j+1)^{\alpha} - (n-j)^{\alpha}\right)$, $0 \le j \le n$.

The error estimation is

$$e = \max\left\{max\left|x_1(t_j) - x_{1h}(t_j)\right|, max\left|x_2(t_j) - x_{2h}(t_j)\right|, \ldots, max\left|x_n(t_j) - x_{nh}(t_j)\right|\right\} = O\left(h^{\rho}\right), \tag{6}$$

where $j = (0,1,2,\ldots, N)$, $\rho = \min\{2, 1+\alpha\}$.

The proposed FO biological disease models, including their state variables, equations, and parameters, are listed in Table 2.

Their dynamical analyses, including equilibrium points, eigenvalues, dynamics, and Lyapunov exponents (LEs) are given in Table 3. The LEs are calculated using the Benettin-Wolf method [45].

The LEs quantify the presence or absence of chaos in the systems. The design of suitable control strategies to stabilise chaos and anticontrol strategies to restore chaos, accordingly, is discussed in Section 3.

3. Design of controllers and anticontrollers

This section is dedicated to the design methodology of controllers in Subsection 3.1 and anticontrollers in Subsection 3.2 as follows.

3.1 Design of controllers to suppress chaos

This subsection presents a discussion of the design of various controller strategies such as BSC, SMC and AFC that have been used to stabilise chaos in disease models of FOEVD, FODM, FOD, and FOHIV.

3.1.1 Back-stepping Control (BSC)—In this method, all the state variables are considered as single separate systems for the integrated systems and each following step is updated subsequently. It has the added advantage of the absence of a derivative term,

which reduces the complexity of the controller, and is efficient when it comes to attaining overall stability.

Theorem 2 [36]: *The stability of a system with a controller defined as* $u = \beta(x)$ *is guaranteed by the Lyapunov function* $V(t, x(t))$ *and its derivative if the following condition is met where* γ *is a class K function.*

$$D^{\alpha}V \leq -\gamma q(x, (\beta(x)))$$

Also, if

$$D^{\alpha}V < -\gamma q(x, \beta(x)),$$

then it can be concluded that the corresponding controller u stabilises the system asymptotically.

Let a disease model be defined as in (2). A controller u is introduced in (2) as shown in (13).

$$D_t^{\alpha} x_i(t) = f_i(X(t), t) + u \tag{13}$$

A set of transformation variables Z_1, Z_2, …, Z_n are defined as in (14):

$$\begin{cases} z_1 = x_1 \\ z_2 = x_2 - \mu_1 \\ \quad . \\ \quad . \\ \quad . \\ z_n = x_n - \mu_{n-1} \end{cases} \tag{14}$$

where μ_1, μ_2, …, μ_{n-1} are independent virtual controllers designed for every subsystem (z_2, z_3, …, z_n), respectively.

The transformation variables defined in (14) are then differentiated in the FO sense as shown in (15).

$$\begin{cases} D^{\alpha} z_1 = D^{\alpha} x_1 \\ D^{\alpha} z_2 = D^{\alpha} x_2 - D^{\alpha} \mu_1 \\ \quad . \\ \quad . \\ \quad . \\ D^{\alpha} z_n = D^{\alpha} x_n - D^{\alpha} \mu_{n-1} \end{cases} \tag{15}$$

A Lyapunov function V_1 is defined as.

$$V_1 = \frac{1}{2} z_1^2 . \tag{16}$$

Using Lemma 1, we have

$$D^{\alpha} V_1 = z_1 D^{\alpha} z_1 \geq \frac{1}{2} D^{\alpha} z_1^2 . \tag{17}$$

Similarly, for the next transformation variable, z_2 in (14), a Lyapunov function V_2 is defined as in (18), from which $D^{\alpha} V_2$ is obtained.

$$V_2 = V_1 + \left(\frac{1}{2}\right) z_2^2 \tag{18}$$

$$D^{\alpha} V_2 = D^{\alpha} V_1 + z_2 D^{\alpha} z_2$$

A suitable value of μ_1 in (15) is to be chosen to satisfy Theorem 2 in the FO sense.

The above steps (16–17) and choice of appropriate values of virtual controllers to satisfy Theorem 2 are continued for all the transformation variables (Z_1, Z_2, …, Z_n) and the back-stepping controller u can be derived.

3.1.2 Sliding Mode Control (SMC)—If a disturbance $l(x_1, x_2, \ldots, x_n, t)$ is present in (2), such that $l(x_1, x_2, \ldots, x_n, t) \leq L > 0$ and bounded, a controller u may be introduced as shown in (19).

$$D_t^{\alpha} x_i(t) = f_i(X(t), t) + l(x_1, x_2, \ldots, x_n, t) + u \tag{19}$$

A sliding variable s is defined as in (20).

$$s = f(x_1, x_2, \ldots, x_n) = x_i + c x_{i-1}, c > 0 \tag{20}$$

For the state variables to converge to equilibrium in the presence of a disturbance, the sliding variable should converge to zero within finite time with the help of the control law.

$$D^{\alpha} s = c D^{\alpha} x_i + l(x_1, x_2, \ldots, x_n) + u \tag{21}$$

The sliding surface in (22) corresponds to a straight line in the state space of the system.

$$s = x_i + c x_{i-1} = 0, c > 0 \tag{22}$$

Using the Lyapunov stability criterion, a Lyapunov function is defined as in (23).

$$V = \frac{1}{2}s^2 \tag{23}$$

For finite time convergence, $D^{\alpha}V$ is modified into (24).

$$D^{\alpha}V < -\kappa V^{\frac{1}{2}}, \kappa > 0 \tag{24}$$

Solving (21) and (23) yields (25):

$$D^{\alpha}V = s(cx_i + l(x_1, x_2, \ldots, x_n) + u). \tag{25}$$

Controller u is proposed as

$$u = -cx_i + v. \tag{26}$$

Replacing u in (25) gives

$$D^{\alpha}V = sl(x_1, x_2, \ldots, x_n) + \quad sv \leq |s|L + sv \quad . \tag{27}$$

Considering $v = -\rho sign(s)$ where $\rho > 0$ and

$$sign(s) = \begin{cases} 1 \; if \; s > 1 \\ 0 \; if \; s = 0 \\ -1 \; if \; s < -1 \end{cases},$$

substituting v in (27), we have,

$$D^{\alpha}V \leq |s|(L - \rho_0) = -\kappa V^{\frac{1}{2}}. \tag{28}$$

Considering equations (23) and (24), then (29) is obtained.

$$D^{\alpha}V = -\kappa V^{\frac{1}{2}} = -\left(\frac{\kappa}{\sqrt{2}}\right)|s|, \kappa > 0 \tag{29}$$

Equation (30) is obtained from (28) and (29).

$$\rho_0 = L + \frac{\kappa}{\sqrt{2}}, \quad \kappa > 0 \tag{30}$$

Thus, the sliding mode controller u is obtained as

$$u = -\left(L + \frac{\kappa}{\sqrt{2}}\right) sign(s) - cx_i, \tag{31}$$

where L, κ, s and c are suitably chosen.

3.1.3 Adaptive Feedback Control (AFC)—Let a disease model be defined as in (2) and rewritten as

$$D_t^{\alpha} x_i(t) = f_i(X(t), t) = Cx + \mathrm{Q}(x)\varsigma \quad , \tag{32}$$

where C is an $n \times n$ constant matrix, $\mathrm{Q}(x) = \mathrm{Q}_{ij}(x)$ denotes a matrix of smooth non-linear functions taking arguments in R^n and $\mathrm{Q}_{ij}(0) = 0$, and ς is the actual parameter vector.

Now, a controller u is introduced in (32) such that the controlled chaotic system becomes

$$D_t^{\alpha} x_i(t) = Cx + \mathrm{Q}(x)\varsigma + u \quad . \tag{33}$$

A matrix D is chosen such that $C + D$ is negative definite, and the control law is given by

$$u = Dx - \mathrm{Q}(x)\hat{\varsigma}, \tag{34}$$

where $\hat{\varsigma}$ is the estimated parameter vector. Substituting u in (33) gives

$$\begin{aligned} &D_t^{\alpha} x_i(t) = Cx + \mathrm{Q}(x)\varsigma + Dx - \mathrm{Q}(x)\hat{\varsigma} \\ &\Rightarrow D_t^{\alpha} x_i(t) = (C + D)x + \mathrm{Q}(x)(\varsigma - \hat{\varsigma}) . \end{aligned} \tag{35}$$

Considering $\hat{\varsigma}$ to asymptotically approach the actual parameter vector ς, (35) becomes (36), which, if Theorem 1 is satisfied, is stable in the FO sense.

$$D_t^{\alpha} x_i(t) = (C + D)x \tag{36}$$

Now, the adaptive feedback controller u can be derived as

$$u = Dx - \mathrm{Q}(x)\varsigma \quad . \tag{37}$$

After successful application of control, the chaotic disease model asymptotically approaches the equilibrium point.

Using the above three control strategies, the different types of controllers obtained for the biological models are listed in Table 4, where u_i is the controller added to control the i^{th} state.

3.2 Design of anticontrollers to generate chaos

This subsection presents three anticontroller strategies based on the LSFAC, SSSFAC and SMAC techniques for introducing chaos in disease models of FOM and FOPI where the presence of chaos inhibits the growth of disease.

3.2.1 Linear State Feedback Anticontrol (LSFAC) Technique—Let the FONLS defined in (2) be that of a non-chaotic disease model. Our aim is to generate chaos in it by anticontrolling it. The Jacobian matrix for (2) at an equilibrium point $(x_1^*, x_2^*, \ldots, x_n^*)$ is

$$\begin{pmatrix} J_{11}J_{12} & \cdots & J_{1n} \\ \vdots & \ddots & \vdots \\ J_{n1}J_{n2} & \cdots & J_{nn} \end{pmatrix}_{x=(x_1^*, x_2^*, \ldots, x_n^*)} = \begin{pmatrix} a_{11} & \cdots & a_{1n} \\ \vdots & \ddots & \vdots \\ a_{n1} & \cdots & a_{nn} \end{pmatrix}_{x=(x_1^*, x_2^*, \ldots, x_n^*)}. \quad (38)$$

A linear state feedback anticontroller, u_a to generate chaos is introduced to (2) as in (39),

$$D_t^{\alpha} x_i(t) = f_i(X(t), t) + u_a, \quad (39)$$

where

$$u_a = Z_1 x_1 + Z_2 x_2 + \cdots + Z_n x_n \quad (40)$$

and $Z_1, Z_2, \ldots, Z_n$ are constant gains.

The Jacobian matrix for (38) at the equilibrium point $(x_1^*, x_2^*, \ldots, x_n^*)$ can now be written as

$$\begin{pmatrix} J_{11}J_{12} & \cdots & J_{1n} \\ \vdots & \ddots & \vdots \\ J_{n1}J_{n2} & \cdots & J_{nn} \end{pmatrix}_{x=(x_1^*, x_2^*, \ldots, x_n^*)} = \begin{pmatrix} a_{11} & \cdots & a_{1n} \\ \vdots & \ddots & \vdots \\ a_{n1} + Z_1 & \cdots & a_{nn} + Z_n \end{pmatrix}_{x=(x_1^*, x_2^*, \ldots, x_n^*)}. \quad (41)$$

Using the Routh-Hurwitz criterion of FO stability analysis in (41), the values of $Z_1, Z_2, \ldots, Z_n$ are suitably chosen such that the system generates positive MLEs and, thereby, chaotic dynamics.

3.2.2 Single State Sinusoidal Feedback Anticontrol (SSSFAC) Technique—A nonlinear feedback anticontroller is given in (42).

$$Km(\omega x, \varphi) = K\begin{pmatrix} m_1(\omega_1 x_1, \varphi_1) \\ m_2(\omega_2 x_2, \varphi_2) \\ \vdots \\ m_n(\omega_n x_n, \varphi_n) \end{pmatrix} \tag{42}$$

Here φ is the upper bound of the anticontroller and ω is the control gain:

$$\begin{cases} \omega = \begin{pmatrix} \omega_1 & 0 & \cdots & 0 \\ 0 & \omega_2 & \cdots & 0 \\ \vdots & \vdots & \ddots & \vdots \\ 0 & 0 & \ldots & \omega_n \end{pmatrix} \\ \varphi = [\varphi_1, \varphi_2, \ldots, \varphi_n]^T \end{cases} . \tag{43}$$

When (42) is added to (2), the anticontrolled system is

$$D_t^{\alpha} x_i(t) = f_i(X(t), t) + Km_i(\omega_i x_i, \varphi_i) \ , \tag{44}$$

where $Km_i(\omega_i x_i, \varphi_i) = \varphi_i sin(\omega_i x_i)$ $(i = 1,2, \ldots, n)$.

Here, K is the control matrix:.

$$K = \begin{pmatrix} k_{11} & k_{12} & \cdots & k_{1n} \\ k_{21} & k_{22} & \cdots & k_{2n} \\ \vdots & \vdots & \ddots & \vdots \\ k_{n1} & k_{n2} & \ldots & k_{nn} \end{pmatrix}. \tag{45}$$

Let the system defined in (2) consist of a linear and a nonlinear subsystem:

$$\begin{cases} D^{\alpha} x_{1,m} = P_{11} x_{1,m} + g(x_{m+1,n}) \\ D^{\alpha} x_{m+1,n} = P_{21} x_{1,m} + P_{22} x_{m+1,n} \end{cases}, \tag{46}$$

where $x_{1,m} = [x_1, x_2, \ldots, x_m]^T$, $x_{m+1,n} = [x_{m+1}, x_{m+2}, \ldots, x_n]^T$, $x = [x_{1,m}, x_{m+1,n}]^T$ and $P_{11}x_{1,m}$, $P_{21}x_{1,m}$ and $P_{22}x_{m+1,n}$ are the linear parts of $f_i(X(t), t)$, $g(x_{m+1,n})$ is the nonlinear part of $f_i(X(t), t)$ and $m = 1,2 \ldots, (n-1)$

For P_{21} defined as

$$P_{21} = \begin{pmatrix} 0 & 0 & \cdots & 0 \\ 0 & 0 & \cdots & 0 \\ \vdots & \vdots & \ddots & \vdots \\ 0 & 0 & \ldots & 0 \end{pmatrix}_{(n-m)\times m}, \tag{47}$$

Equation (46) can be re-written as below.

$$\begin{cases} D^{\alpha}x_{1,m} = P_{11}x_{1,m} + g\left(x_{m+1,n}\right) \\ D^{\alpha}x_{m+1,n} = P_{22}x_{1,m} \end{cases} \tag{48}$$

Solving (44) and (48) yields

$$\begin{cases} D^{\alpha}x_{1,m} = P_{11}x_{1,m} + g\left(x_{m+1,n}\right) \\ D^{\alpha}x_{m+1,n} = P_{22}x_{m+1,n} + K_{21}m\left(\omega_{1,m}x_{1,m}, \varphi_{1,m}\right) \end{cases}, \tag{49}$$

where K_{21} is a sub-matrix of the control matrix K and is expressed as

$$K = \begin{pmatrix} k_{11} & k_{12} & \cdots & k_{1n} \\ k_{21} & k_{22} & \cdots & k_{2n} \\ \vdots & \vdots & \ddots & \vdots \\ k_{n1} & k_{n2} & \ldots & k_{nn} \end{pmatrix} = \begin{pmatrix} K_{11} & K_{12} \\ K_{21} & K_{22} \end{pmatrix}_{n\times n}. \tag{50}$$

Here,

$$\begin{cases} K_{11} = \begin{pmatrix} 0 & 0 & \cdots & 0 \\ 0 & 0 & \cdots & 0 \\ \vdots & \vdots & \ddots & \vdots \\ 0 & 0 & \ldots & 0 \end{pmatrix}_{m\times m} \\ K_{12} = \begin{pmatrix} 0 & 0 & \cdots & 0 \\ 0 & 0 & \cdots & 0 \\ \vdots & \vdots & \ddots & \vdots \\ 0 & 0 & \ldots & 0 \end{pmatrix}_{m\times(n-m)} \\ K_{21} = \begin{pmatrix} k_{m+1,1} & k_{m+1,2} & \cdots & k_{m+1,n} \\ k_{m+2,1} & k_{m+2,2} & \cdots & k_{m+2,n} \\ \vdots & \vdots & \ddots & \vdots \\ k_{n1} & k_{n2} & \cdots & k_{nn} \end{pmatrix}_{(n-m)\times m} \\ K_{22} = \begin{pmatrix} 0 & 0 & \cdots & 0 \\ 0 & 0 & \cdots & 0 \\ \vdots & \vdots & \ddots & \vdots \\ 0 & 0 & \ldots & 0 \end{pmatrix}_{(n-m)\times(n-m)} \end{cases}$$

and the anticontroller $m(\omega_{1,m}x_{1,m}, \varphi_{1,m})$ in (49) is expressed as

$$m\left(\omega_{1,m}x_{1,m}, \varphi_{1,m}\right) = \begin{pmatrix} m_1(\omega_1 x_1, \varphi_1) \\ m_2(\omega_2 x_2, \varphi_2) \\ \vdots \\ m_m(\omega_m x_m, \varphi_m) \end{pmatrix}, \tag{51}$$

where $\varphi_{1,m} = [\varphi_1, \varphi_2, \ldots, \varphi_m]^T$ and $\omega = \begin{pmatrix} \omega_1 & 0 & \cdots & 0 \\ 0 & \omega_2 & \cdots & 0 \\ \vdots & \vdots & \ddots & \vdots \\ 0 & 0 & \ldots & \omega_n \end{pmatrix}$.

Theorem 3. [41]: *If the real part of all eigenvalues of the submatrices P_{11} and P_{22} in* (49) *have negative real part, the nonlinear controller $m(\omega_{1,m}x_{1,m}, \varphi_{1,m})$ is uniformly bounded:*

$$sup_{0 \le t < \infty} \left\| m(\omega_{1,m}x_{1,m}, \varphi_{1,m}) \right\| \le \|\varphi_{1,m}\| < \infty$$

and $g(x_{m+1,n})$ is a bounded-input/bounded-output function satisfying

$$\left\| g(x_{m+1,n}) \right\| \le M_1 < \infty \left(if \ \|x_{m+1,n}\| \le M_2 < \infty \right),$$

where $\|\cdot\|$ is the Euclidean norm, then (49) is globally bounded.

Theorem 4. [41]: *If the following conditions are satisfied, then the system* (49) *is chaotic while being globally bounded.*

- **i.** *The nonlinear controller $m(\omega_{1,m}x_{1,m}, \varphi_{1,m})$ is uniformly bounded:*

$$sup_{0 \le t < \infty} \left\| m(\omega_{1,m}x_{1,m}, \varphi_{1,m}) \right\| \le \|\varphi_{1,m}\| < \infty$$

- **ii.** *The nonlinear function $g_{(m+1,n)}$ is of bounded-input/bounded-output:*

$$\left\| g(x_{m+1,n}) \right\| \le M_1 < \infty \left(if \|x_{m+1,n}\| \le M_2 < \infty \right)$$

- **iii.** *All eigenvalues of the two sub-matrices P_{11} and P_{22} have negative real parts.*
- **iv.** All equilibria, say Q, of system (49) are saddle-foci.
- **v.** The anticontrolled system (49) has positive Lyapunov exponents.
- **vi.** *The Jacobian of the controlled system at an equilibrium Q is*

$$J_0 = \begin{pmatrix} J_{11}J_{12} & \cdots & J_{1n} \\ \vdots & \ddots & \vdots \\ J_{n1}J_{n2} & \cdots & J_{nn} \end{pmatrix}_{x=0} =$$

$$\begin{pmatrix} a_{11} & \cdots & a_{1m} & \frac{\partial g_1(x_{m+1,n})}{\partial x_{m+1}} & \cdots & \frac{\partial g_1(x_{m+1,n})}{\partial x_n} \\ \vdots & \ddots & \vdots & \vdots & \ddots & \vdots \\ a_{m1} & \cdots & a_{mm} & \frac{\partial g_m(x_{m+1,n})}{\partial x_{m+1}} & \cdots & \frac{\partial g_m(x_{m+1,n})}{\partial x_n} \\ k_{m+1,1}\frac{\partial m_1(\omega_1 x_1, \varphi_1)}{\partial x_1} & \cdots & k_{m+1,m}\frac{\partial m_m(\omega_m x_m, \varphi_m)}{\partial x_m} & a_{m+1,m+1} & \cdots & a_{m+1,n} \\ \vdots & \ddots & \vdots & \vdots & \ddots & \vdots \\ k_{n1}\frac{\partial m_1(\omega_1 x_1, \varphi_1)}{\partial x_1} & \cdots & k_{nm}\frac{\partial m_m(\omega_m x_m, \varphi_m)}{\partial x_m} & a_{n,m+1} & \cdots & a_{nn} \end{pmatrix}_Q$$

with diagonal elements satisfying:

$$\sum_{i=1}^{n} J_{ii}(Q) < 0.$$

If (44) satisfies the given Theorems 3 and 4, then the designed single-state sinusoidal anticontroller may introduce chaos into the disease model.

3.2.3 Sliding Mode Anticontrol (SMAC) Technique—The SMC defined in (31) as discussed in subsection 3.1.2 has been used here as an anticontroller to induce chaos by choosing appropriate values of the parameters L, κ, s and c.

Using the aforementioned three anticontrol strategies, the anticontrollers obtained for the disease models are listed in Table 5, where the anticontroller u_{ai} is added to anticontrol the i^{th} state of the disease model.

4. Results and Discussion

The previous sections deal with FO biological models of diseases along with the design of controllers and anticontrollers. We now discuss the observations made subsequently with their application to the respective disease models in this section.

4.1 Investigation of chaos in the proposed FO disease models and controlling chaos

The chaotic attractors of the diseases FOEVD, FODM, FOHIV and FOD prior to application of controllers are illustrated in Fig. 1. A representative bifurcation diagram of FOEVD against the FO parameter α is plotted in Fig. 2, where it is seen that the system is stable for $\alpha < 0.992$ and becomes chaotic when $\alpha \in [0.992,1]$. The attractors and the bifurcation analysis in Figs. 1–2 are in agreement with the LEs of the FO models of the diseases already listed in Table 3 and show that they display chaos in their fractional dynamics when in the diseased regime.

The observations pertaining to the respective disease models after the application of controllers to suppress chaos are listed in Table 6. Here, the column ‘state’ represents the number of states of the disease model where the controller is added.

The negative MLEs in Table 6 and the corresponding stabilised time trajectories, as illustrated in Figs. 3–6, imply the successful design of the controllers in suppressing chaos.

4.2 Investigation of chaos in the proposed FO disease models and anticontrolling chaos

This subsection pertains to the application of anticontrollers to those biological models where absence of chaos indicates a diseased state. Hence, the presence of chaos in them is investigated after anticontrol. As shown in Table 7, a positive MLE in each disease phase after addition of anticontrollers confirms the generation of chaos.

The corresponding time trajectories after chaos anticontrol are shown in Figs. 7–8.

The phase portraits of the diseases after anticontrol display chaotic attractors, as shown in Fig. 9. A bifurcation diagram of FOM against the FO parameter α is plotted in Fig. 10, where it is seen that on adding LSFAC, the previously stable disease model now generates chaos for the range $\alpha \in [0.87, 1]$.

While suppressing chaos, as presented in Table 6, though AFC performs better than BSC and SMC in terms of settling time, it is to be noted that AFC uses more controllers added to multiple states of the disease model, indicating greater control effort. The advantage of SMC is that it is robust to uncertain disturbances, whereas BSC uses lesser control effort, although

they take more time to settle. Amongst anticontrol strategies, except LSFAC applied to FOM, the rest are all single state anticontrollers, simple in design and easy to implement.

5 Conclusion

This paper accomplishes the following significant goals.

First, is the investigation of chaos in fractional-order (FO) biological models of FO Ebola Virus, FO Diabetes Mellitus, FO HIV and FO Dengue, where presence of chaos enhances the propagation of the disease and is therefore undesirable. Chaos causes tremendous sensitivity to initial conditions of physical factors and unpredictability, abnormal secretion of insulin in blood, increases the rate of virus replication and measure of infectiousness in the above FO models, respectively. Control design strategies, using back-stepping control, sliding mode control and adaptive feedback control are proposed in the work. On applying the proposed controllers to the biological models, it is concluded that chaos dies out efficiently so that normal functioning can be restored.

Second, is the proposal of FO models of Migraine and Parkinson's diseases where the absence of chaos indicates the onset of diseases. Lack of chaos hampers the basal excitability of brain neurons leading to the above neurological disorders. Anti control strategies using Linear State Feedback Anticontrol, Single State Sinusoidal Feedback Anticontrol and Sliding Mode Anticontrol are proposed whose application to the biological models, successfully generates chaos to enable healthy functioning

This work also establishes a comparative study on the designed controllers and anticontrollers to draw conclusion on the suitability of their application as required. Analysis of chaos in incommensurate FO models is left as a future scope of work. As the objectives of this paper have been successfully achieved, hence the work will prove useful for biomedical applications and diagnosis.

Acknowledgment

This work is supported by the Research and Innovation Grant, Tezpur University, India under sanction no. TU/Fin/R/18-19/339.

References

[1]. Borah M, Roy BK. Systematic construction of high dimensional fractional-order hyperchaotic systems. Chaos, Solitons and Fractals 2019;doi:10.1016/j.chaos.2019.109539.

[2]. Borah M On coexistence of fractional-order hidden attractors. Journal of Computational and Nonlinear Dynamics, American Society of Mechanical Engineers (ASME) 2018;13:090906–090917.

[3]. Korolj A, Wu H-T, Radisic M. A healthy dose of chaos: Using fractal frameworks for engineering higher-fidelity biomedical systems. Biomaterials 2019;219:119363. [PubMed: 31376747]

[4]. Aguiar M, Kooi BW, Stollenwerk N. Multi-strain deterministic chaos in dengue epidemiology, a challenge for computational mathematics. Numerical Analysis and Applied Mathematics International conference 2009;2:CP1168.

[5]. Tene AG, Tchoffo M, Tabi BC, Kofane TC. Generalized synchronization of regulate seizures dynamics in partial epilepsy with fractional-order derivatives. Chaos, Solitons and Fractals 2020;132:109553.

[6]. Das DK, Khajanchi S, Kar TK. Transmission dynamics of tuberculosis with multiple re-infections. Chaos, Solitons and Fractals 2020;132:109450.

[7]. Panahi S, Shirzadian T, Jalili M, Jafari S. A new chaotic network model for epilepsy. Applied Mathematics and Computation 2019;346:395–407.

[8]. Fahimi M, Nouri K, Torkzadeh L. Chaos in a stochastic cancer model. Physica A 2019;doi:10.1016/j.physa.2019.123810.

[9]. Nudee K, Chinviriyasit S, Chinviriyasit W. The effect of backward bifurcation in controlling measles transmission by vaccination. Chaos, Solitons and Fractals 2019;123:400–412.

[10]. Jan R, Khan MA, Kumam P, Thounthong P. Modeling the transmission of dengue infection through fractional derivatives. Chaos, Solitons and Fractals 2019;127:189–216.

[11]. Shaikh AS, Nisar KS. Transmission dynamics of fractional order typhoid fever model using Caputo–Fabrizio operator. Chaos, Solitons and Fractals 2019;128:355–365.

[12]. Berhe HW, Qureshi S, Shaikh AA. Deterministic modeling of dysentery diarrhoea epidemic under fractional Caputo differential operator via real statistical analysis. Chaos, Solitons and Fractals 2019;doi:10.1016/j.chaos.2019.109536.

[13]. Zheng T, Nie LF, Teng Z, Luo Y. Competitive exclusion in a multi-strain malaria transmission model with incubation period. Chaos, Solitons and Fractals 2019;doi:10.1016/j.chaos.2019.109545.

[14]. Shabestari PS, Panshi S, Hatef B, Jafari S, Sprott JC. A new chaotic model for glucose-insulin regulatory system. Chaos, Solitons and Fractals 2018;112:44–51.

[15]. Bayani A, Jafari S, Sprott JC, Hatef B. A chaotic model of migraine headache considering the dynamical transitions of this disease. Non-linear Dynamics and Chaos 2018;123:1–6.

[16]. Salman SM, Ahmed E. A mathematical model for Creutzfeldt Jacob Disease (CJD). Chaos, Solitons and Fractals 2018;116:249–260.

[17]. Agusto FB, Khan MA. Optimal control strategies for dengue transmission in Pakistan. Mathematical Biosciences 2018;305:102–121. [PubMed: 30218686]

[18]. Liu Q, Jiang D, Hayat T, Alsaedi A. Dynamics of a stochastic tuberculosis model with antibiotic resistance. Chaos, Solitons and Fractals 2018;109:223–230.

[19]. Valle PA, Coria LN, Gamboa D, Plata C. Bounding the Dynamics of a chaotic-cancer mathematical model. Mathematical Problems in Engineering 2018;9787015.

[20]. Baba IA, Hincal E. A model for influenza with vaccination and awareness. Chaos, Solitons and Fractals 2018;106:49–55.

[21]. Peter OJ, Afolabi OA, Victor AA, Akpan CE, Oguntolu FA. Mathematical model for the control of measles., J. Appl. Sci. Environ. Manage 2018;22:571–576.

[22]. Bairagi N, Adak D. Dynamics of cytotoxic T-lymphocytes and helper cells in human immunodeficiency virus infection with hill-type infection rate and sigmoidal CTL expansion. Chaos, Solitons and Fractals 2017;103:52–67.

[23]. Belozyotov VY, Zaytsev VG. Mathematical modelling of parkinson's illness by chaotic dynamics methods. Problems on mathematical modelling and the theory of differentials equations 2017;9:21–39.

[24]. Tilahun GT, Makinde OD, Malonza D. Modeling and optimal control of typhoid fever disease with cost-effective strategies. Computational and Mathematical Methods in Medicine 2017;2324518. [PubMed: 29081828]

[25]. Mangiarott S, Peyre M, Huc M. A chaotic model for the epidemic of ebola virus disease in West Africa(2013–2016). Chaos 2016;26:1–15.

[26]. Zhang F, Li J, Zheng C, Wang L. Dynamics of an HBV/HCV infection model with intracellular delay and cell proliferation. Communications in Nonlinear Science and Numerical Simulation 2017;42:464–476.

[27]. Lemos-Paiao AP, Silva CJ, Torres DFM. An epidemic model for cholera with optimal control treatment., Journal of Computational and Applied Mathematics 2016; doi:10.1016/j.cam.2016.11.002.

[28]. Patel AJ, Prajapati MB, Bhathawala PH. Mathematical modeling of swine flu (H1N1) disease. IOSR Journal of Mathematics 2016;12:10–14.

[29]. Gkana A, Zachilas L. Bifurcations and chaos in discrete time gonorrhoea model. Chaotic modelling and simulation 2015;1:51–64.

[30]. Mangiarotti S Low dimensional chaotic models for the plague epidemic in Bombay (1896–1911). Chaos, Solitons and Fractals 2015;81:184–196.

[31]. Itik M, Banks SP. Chaos in a three-dimensional cancer model. International Journal of Bifurcation and Chaos 2010;20:71–79.

[32]. Schnog JB, Duits AJ, Muskiet FA, ten Cate H, Rojer RA, Brandjes DP. Sickle cell disease; a general overview. PubMed: United States National Library of Medicine 2004;62:364–374.

[33]. Kocamaz UE, Cevher B, Uyaroglu Y. Control and synchronization of chaos with sliding mode control based on cubic reaching rule. Chaos, solitons, and fractals 2017;105:92–98.

[34]. Louridas GE, Louridas AG. Impact of chaos in progression of heart failure. International journal of applied science and technology 2012;2.

[35]. Gurbani C, Kumar V. Designing robust control by sliding mode control technique. Advance in Electronic and Electric Engineering 2013;3:137–144.

[36]. Shukla MK, Sharma BB, Azar AT. Control and synchronization of a fractional order hyperchaotic system via backstepping and active backstepping approach. Mathematical techniques of fractional order systems 2018;559–595.

[37]. Agrawal SK, Srivastava M, Das S. Synchronization of fractional order chaotic systems using active control method. Chaos, solitons, and fractals 2012;45:737–752.

[38]. Vaidyanathan S Adaptive design of controller and synchroniser for Lu-Xiao chaotic system with unknown parameters. International Journal of Computer Science and Information Technology 2013;5:197–210.

[39]. Welsh AJ, Delgado C, Trimble CL, Kaboudian A, Fenton FH. Simulating waves, chaos and synchronization with a microcontroller. Chaos 2019;29:doi:10.1063/1.5094351.

[40]. He J, Yu S, Cai J. Topological horseshoe analysis for a three dimensional anti-control system and its application. Optik 2016;127:9444–9456.

[41]. Yu S, Chen G. Chaotifying continuous-time nonlinear autonomous system. Int. J. Bifurcation and Chaos 2012;22:1250232.

[42]. Borah M, Roy BK. Design of Fractional-order Hyperchaotic Systems with Maximum Number of Positive Lyapunov Exponents and Their Antisynchronisation using Adaptive Control. International Journal of Control 2018; 91: 2615–2630.

[43]. Aguila-Camacho N, Duarte-Mermoud MA, Gallegos JA. Lyapunov functions for fractional order systems. Commun Nonlinear Sci Numer Simulat 2014;19:2951–2957.

[44]. Diethelm K, Ford NJ, Freed AD. A predictor-corrector approach for the numerical solution of fractional differential equations. Nonlinear Dynamics 2002;29:3–22.

[45]. Danca MF, Kuznetsov N. Matlab code for Lyapunov exponents of fractional order systems. International Journal of Bifurcation and Chaos 2018;28:1850067.

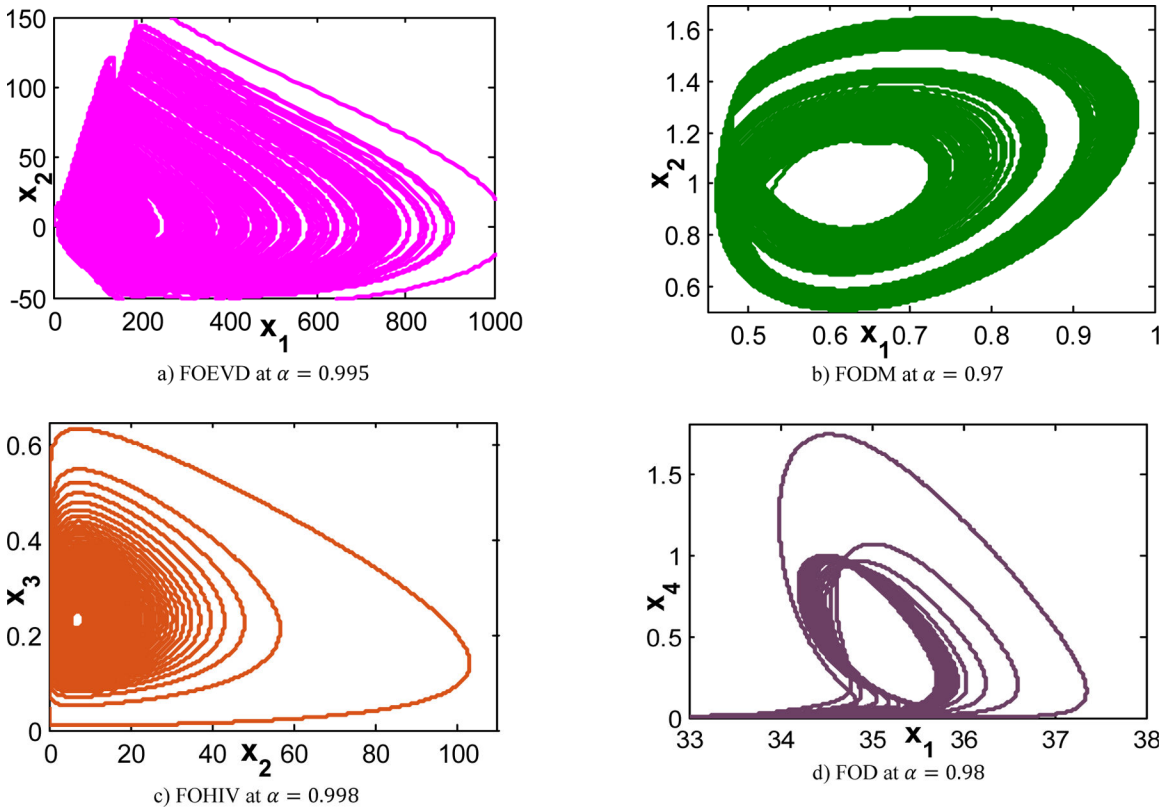

Fig. 1.

Chaotic attractors of proposed FO models of biological systems in their diseased phase, before chaos suppression

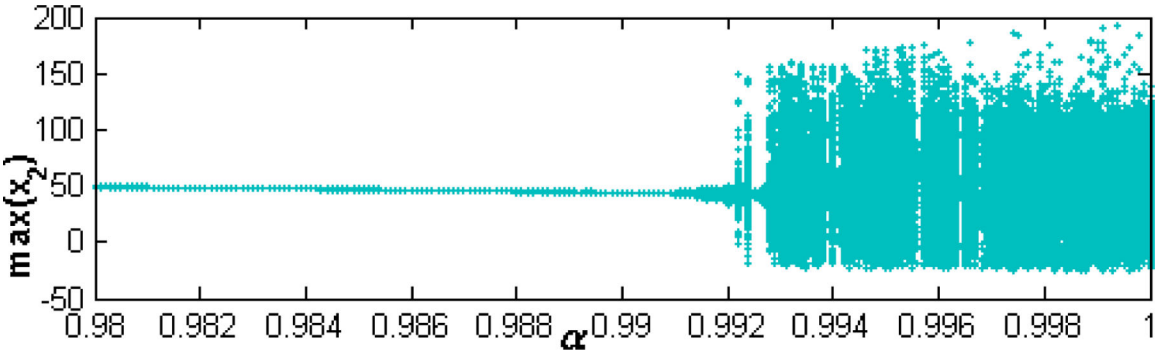

Fig. 2.

Bifurcation diagram of FOEVD against the FO bifurcation parameter α, before chaos suppression

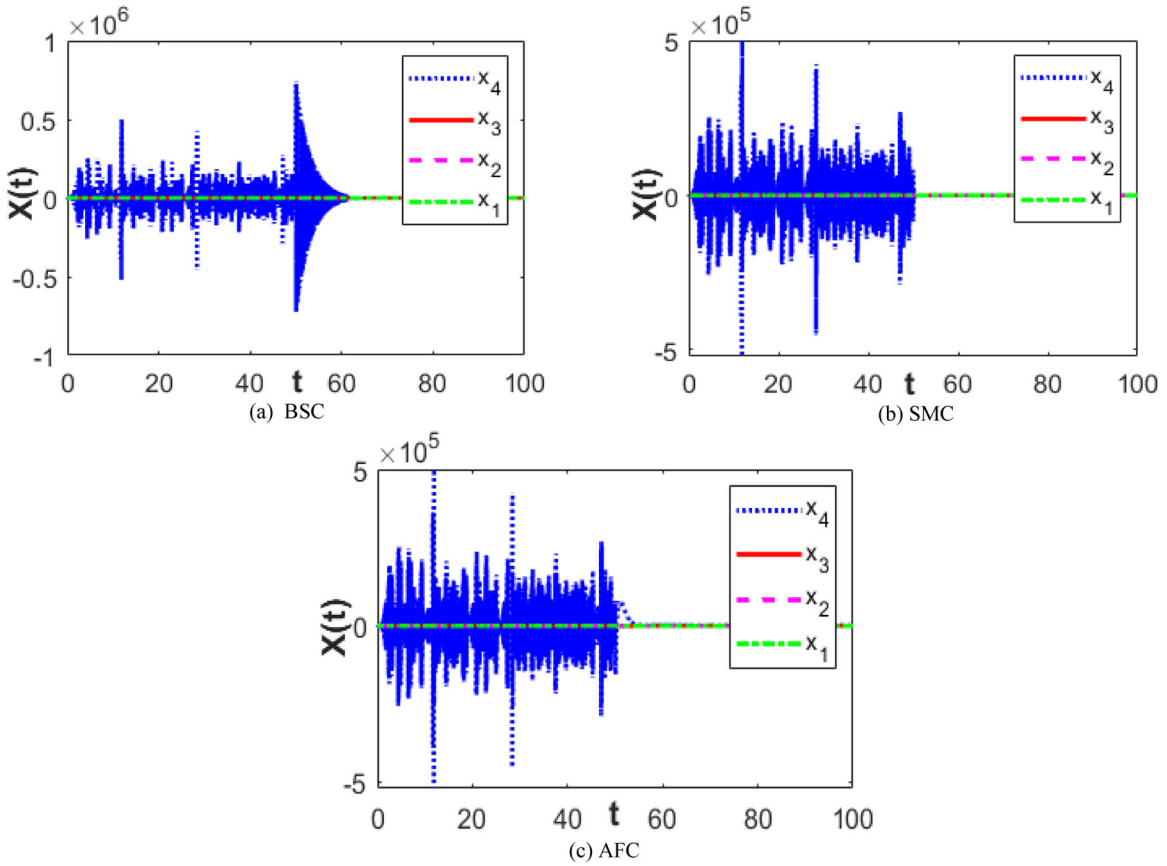

Fig. 3.

Time series plot of FOEVD with proposed controllers for suppressing chaos added at 50s.

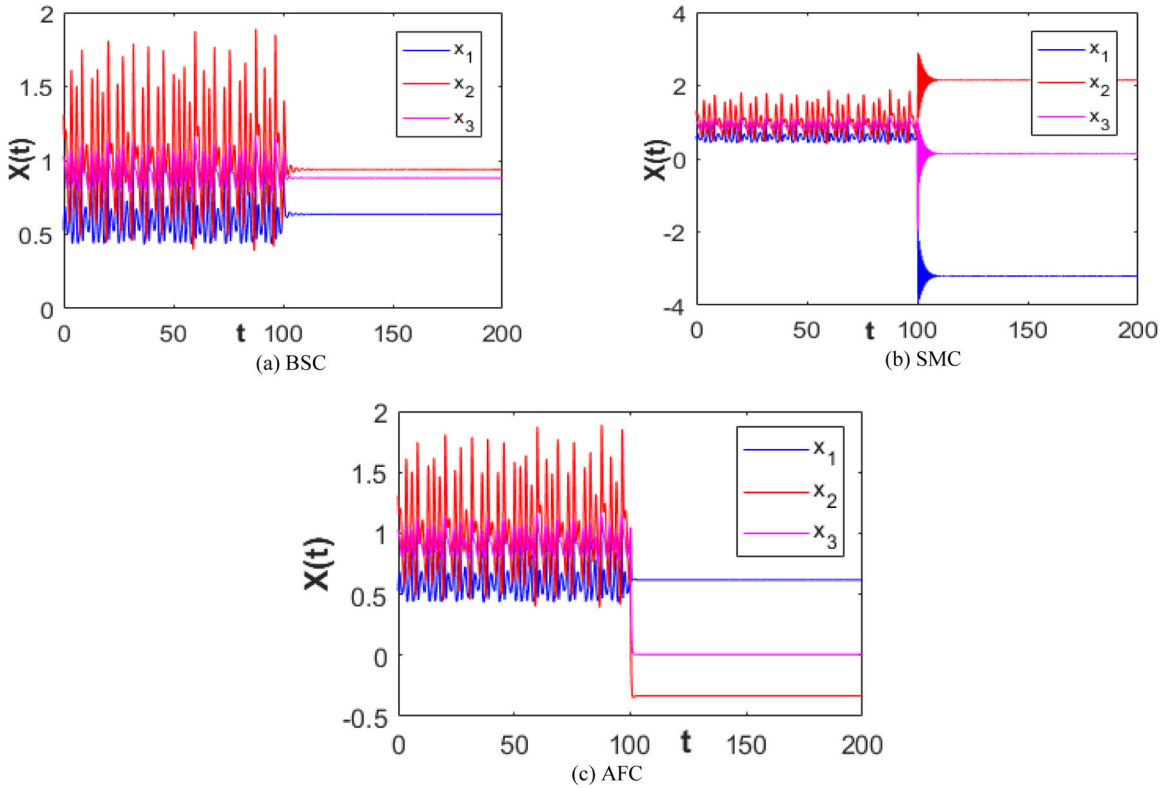

Fig. 4.
Time series plot of FODM with proposed controllers for suppressing chaos added at 100s.

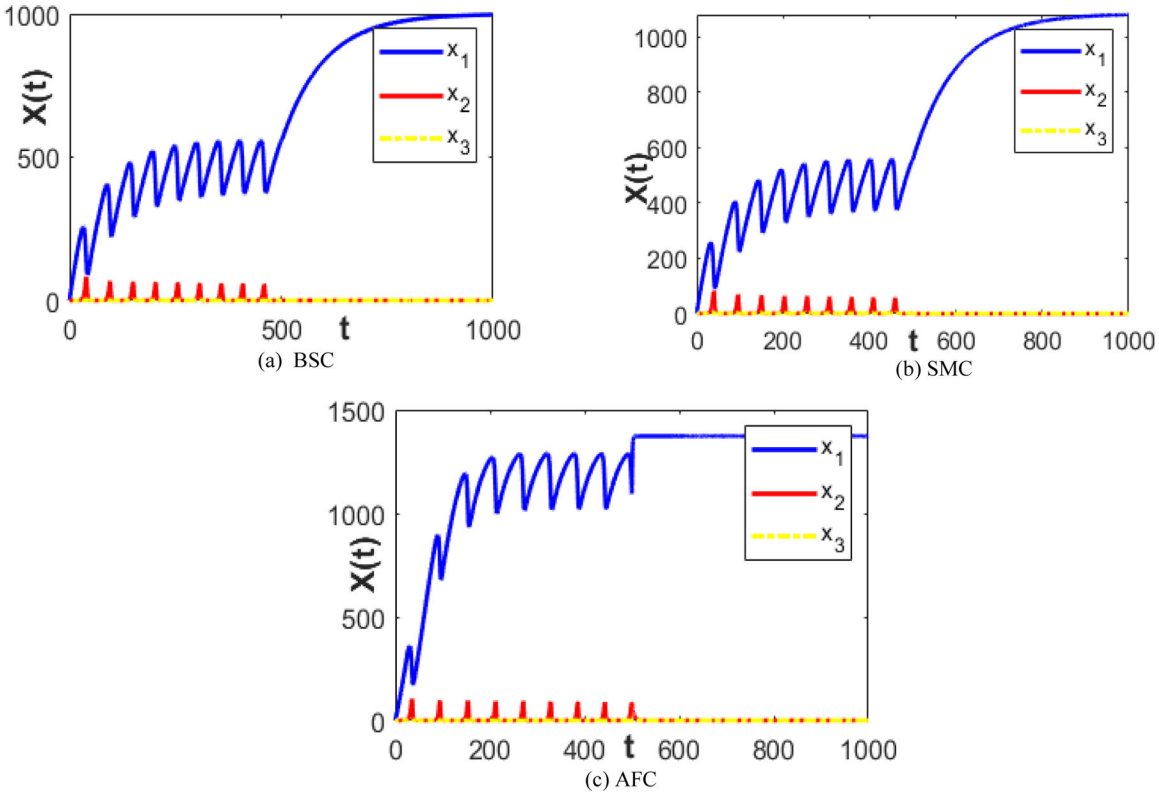

Fig. 5.

Time series plot of FOHIV with proposed controllers for suppressing chaos added at 500s.

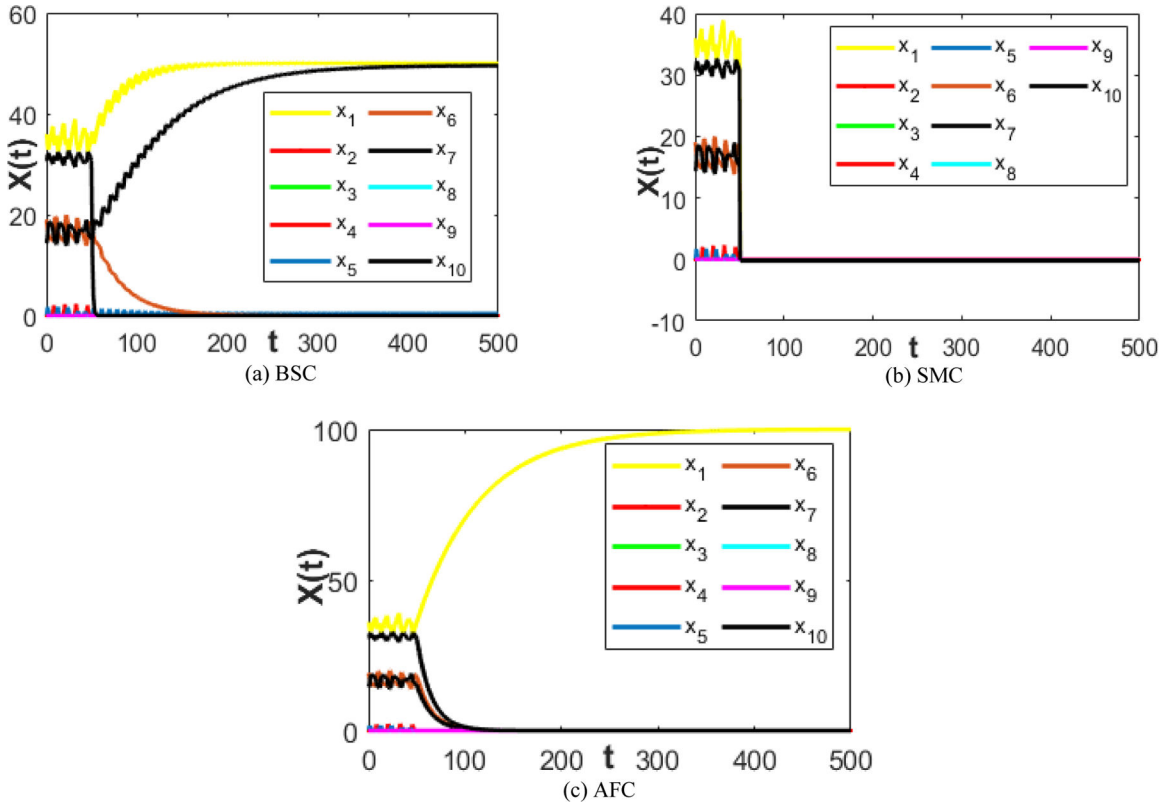

Fig. 6.
Time series for FOD with proposed controllers for suppressing chaos added at 50s.

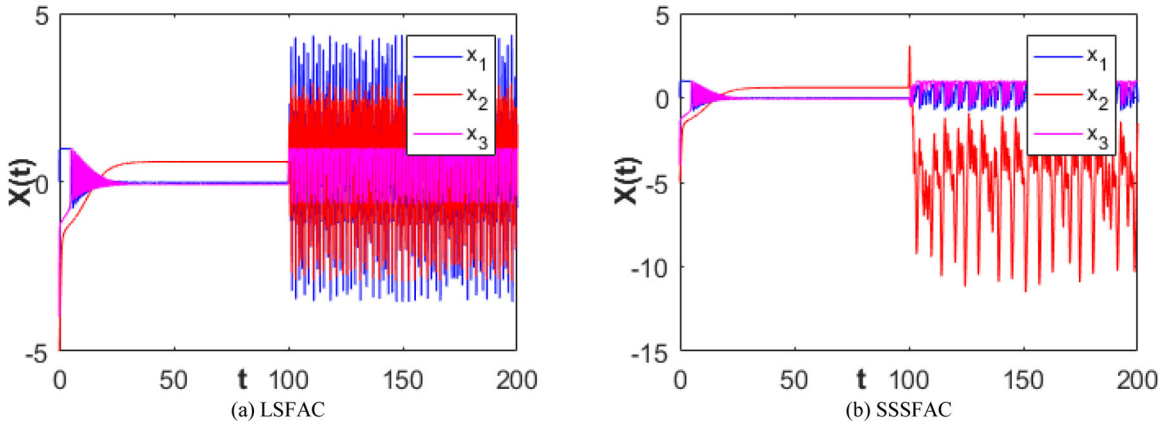

Fig. 7.

Time series of FOM where proposed anticontrollers for generating chaos are added at 100s

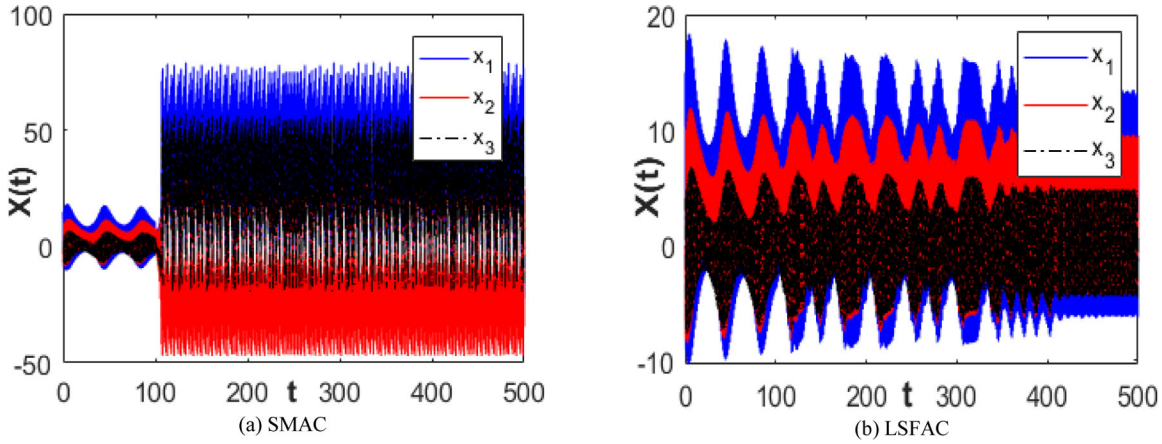

Fig. 8.

Time series of FOPI where proposed anticontrollers for generating chaos are added at 100s

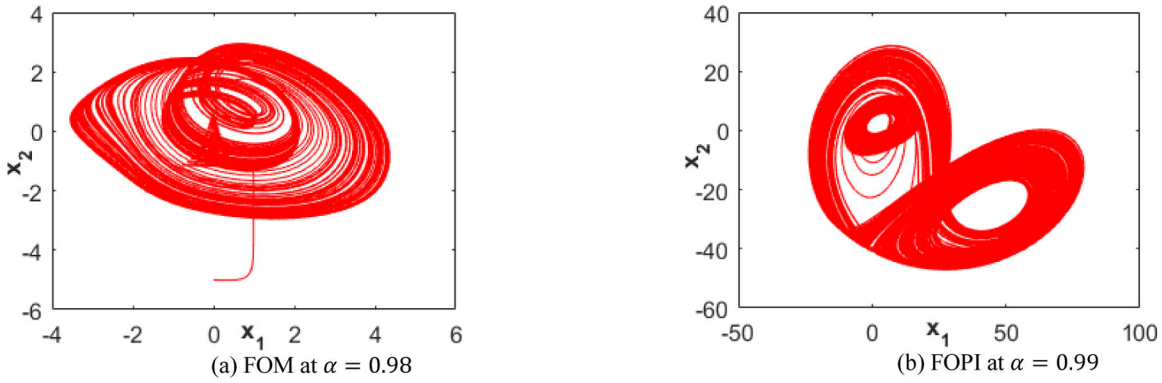

(a) FOM at $\alpha = 0.98$ (b) FOPI at $\alpha = 0.99$

Fig. 9.
Chaotic attractors in disease models after anticontrol

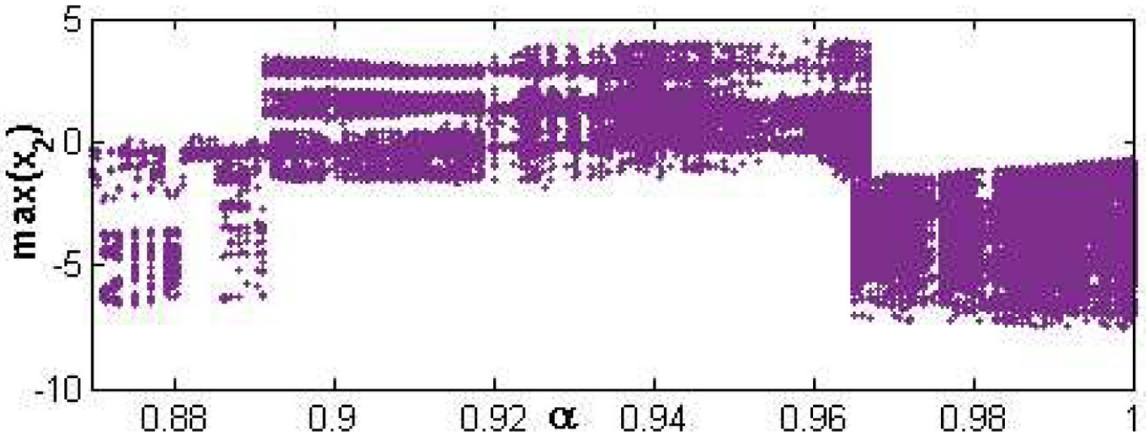

Fig. 10.
Bifurcation diagram of FOM against the FO bifurcation parameter a after anticontrol

Table 1:

List of works on recent chaotic models of diseases

Sl. No.	Works	Year	Disease	Integral Order model	Fractional Order model	Control method
1.	Tene et al. [5].	2020	Epilepsy	No	Yes	Ge-Yao-Chen partial region stability theory
2.	Das et al. [6].	2020	Tuberculosis	Yes	No	Not done
3.	Panahi et al. [7].	2019	Epilepsy	Yes	No	Not done
4.	Fahimi et al. [8].	2019	Cancer	Yes	No	Not done
5.	Nudee et al. [9].	2019	Measles	Yes	No	Not done
6.	Jan et al. [10].	2019	Dengue	No	Yes	Not done
7.	Shaikh et al. [11].	2019	Typhoid	No	Yes	Not done
8.	Berhe et al. [12].	2019	Diarrhoea	No	Yes	Not done
9.	Zheng et al. [13].	2019	Malaria	Yes	No	Not done
10.	Shabestari et al. [14].	2018	Diabetes	Yes	No	Not done
11.	Bayani et al. [15].	2018	Migraine	Yes	No	Not done
12.	Salman et al. [16].	2018	Creutzfeldt Jacob Disease	Yes	No	Not done
13.	Agusto et al. [17].	2018	Dengue	Yes	No	Optimal Control
14.	Liu et al. [18].	2018	Tuberculosis	Yes	No	Not done
15.	Valle et al. [19].	2018	Cancer	Yes	No	Not done
16.	Baba et al. [20].	2018	Influenza	Yes	No	Not done
17.	Peter et al. [21].	2018	Measles	Yes	No	Not done
18..	Bairagi et al. [22].	2017	HIV	Yes	No	Not done
19.	Belozyorov et al. [23].	2017	Parkinson’s illness	Yes	No	Not done
20.	Tilahun et al. [24].	2017	Typhoid	Yes	No	Optimal Control
21.	Mangiarotti et al. [25].	2016	Ebola Virus Disease	Yes	No	Not done
22.	Zhang et al. [26].	2016	Hepatitis	Yes	No	Not done
23.	Lemos-Paiao et al. [27].	2016	Cholera	Yes	No	Optimal Control
24.	Patel et al. [28].	2016	Swine flu	Yes	No	Not done
25.	Gkana et al. [29].	2015	Gonorrhoea	Yes	No	Not done
26.	Mangiarotti S [30].	2015	Plague	Yes	No	Not done
27.	Itik et al. [31].	2010	Cancer	Yes	No	Not done
28.	Aguiar et al. [4].	2009	Dengue	Yes	No	Not done
29.	Schnog et al. [32].	2004	Sickle Cell	Yes	No	Not done

Table 2:

Proposed fractional-order disease models

Sl. no.	Disease	Model	α	Parameters	Denotations
1.	Fractional-order Ebola Virus Disease (FOEVD)	$\begin{cases} D^{\alpha}x_1 = b_1x_2x_4 + b_2{x_2}^2 - b_3x_1x_2 \\ D^{\alpha}x_2 = x_3 \\ D^{\alpha}x_3 = x_4 \\ D^{\alpha}x_4 = b_4 + þb_5x_4 + b_6{x_4}^2 - b_7x_3 - b_8{x_3}^2 + b_9x_2 - b_{10}x_2x_4 + b_{11}x_2x_3 - b_{12}{x_2}^2 - b_{13}x_1 - b_{14}x_1x_4 - b_{15}x_1x_3 + b_{16}x_1x_2 + b_{17}{x_1}^2 \end{cases}$ (7)	0.992	b_1 = 1.0894896 × 10^{-4}, b_2 = 1.4135051035, b_3 0.9815931187, b_4 = 5791.076327, b_5 = 3.744720590, b_6 = 2.2511395 × 10^{-5}, b_7 = 1921.271852, b_8 = 0.1614398401, b_9 = 34650.56048, b_{10} = 0.057295177, b_{11} = 14.52947493, b_{12} = 1056.142579, b_{13} = 17867.66051, b_{14} = 0.06616088061,; b_{15} = 24.91575291, b_{16} 300.3855818, b_{17} = 179.1636118, þ = 1	x_1, x_2, x_3 and x_4 denote the two time series of the number of infected and number of resultant deaths, and the first and second time derivative of the time series of number of deaths, respectively.
2.	Fractional-order Diabetes Mellitus (FODM) (Glucose Insulin regulator system)	$\begin{cases} D^{\alpha}x_1 = -w_1x_1 + w_2x_1x_2 + w_3{x_2}^2 + w_4{x_2}^3 + w_5x_3 + w_6{x_3}^2 w_7{x_3}^3 + w_{20} \\ D^{\alpha}x_2 = w_8x_1x_2 + w_9{x_1}^2 - w_{10}{x_1}^3 + w_{11}x_2(1-x_2) - w_{12}x_3 - w_{13}{x_3}^2 - w_{14}{x_3}^3 + w_{21} \\ D^{\alpha}x_3 = w_{15}x_2 + w_{16}{x_2}^2 + w_{17}{x_2}^3 + w_{18}x_3 - w_{19}x_2x_3 \end{cases}$ (8)	0.97	w_1 = 2.04, w_2 = 0.1, w_3 = 1.09, w_4 = −1.08, w_5 = 0.03, w_6 = −0.06, w_7 = 2.01, w_8 = 0.22, w_9 = −3.84, w_{10} = −1.2, w_{11} = 0.3, w_{12} = 1.37, w_{13} = −0.3, w_{14} = 0.22, w_{15} = 0.3, w_{16} = −1.35, w_{17} = 0.5, w_{18} = −0.42, w_{19} = −0.15, w_{20} = −0.19, w_{21} = −0.56	x_1, x_2, and x_3 represent the concentrations of insulin, glucose and β-cells, respectively.

Sl. no.	Disease	Model	a	Parameters	Denotations
3.	Fractional-order Human Immunodeficiency Virus (FOHIV) infection	$\begin{cases} D^{\alpha}x_1 = -\frac{\beta_0 d_3 \delta}{\gamma_0}\left(\frac{{x_1}^{n_0}x_2}{{d_1}^{n_0}+{x_1}^{n_0}}\right)+s_0-\mu x_1+rx_1\left(1-\frac{x_1}{k}\right) \\ D^{\alpha}x_2 = \frac{\beta_0 d_3 \delta}{\gamma_0}\left(\frac{{x_1}^{n_0}x_2}{{d_1}^{n_0}+{x_1}^{n_0}}\right)-(\delta+\mu)x_2-p_0x_2x_3 \\ D^{\alpha}x_3 = \left(\frac{q_0x_2x_3}{\epsilon x_3+1}\right)-d_2x_3 \end{cases}$ (9)	0.998	d_1 = 120, d_2 = 0.07, d_3 = 400, p_0 = 2.5, q_0 = 0.01, δ = 0.26, β_0 = 0.027, γ_0 = 3, μ = 0.01, r = 0.032, k = 1500, ϵ = 0.001, n_0 = 1, s_0 = 10	x_1, x_2 and x_3, respectively signify the concentration of uninfected CD4$^+$ cells, concentration of infected CD4$^+$ cells and CTL concentration at time t.
4.	Fractional-order Dengue (FOD)	$\begin{cases} D^{\alpha}x_1 = -\left(\frac{e_0}{N_0}\right)x_1(x_2+Bx_9)-\left(\frac{e_0}{N_0}\right)x_1(x_3+Bx_8)+B_0(N_0-x_1) \\ D^{\alpha}x_2 = \left(\frac{e_0}{N_0}\right)x_1(x_2+Bx_9)-(d+B_0)x_2 \\ D^{\alpha}x_3 = \left(\frac{e_0}{N_0}\right)x_1(x_3+Bx_8)-(d+B_0)x_3 \\ D^{\alpha}x_4 = dx_2-(a+B_0)x_4 \\ D^{\alpha}x_5 = dx_3-(a+B_0)x_5 \\ D^{\alpha}x_6 = -\left(\frac{e_0}{N_0}\right)x_6(x_3+Bx_8)+ax_4-B_0x_6 \\ D^{\alpha}x_7 = -\left(\frac{e_0}{N_0}\right)x_7(x_2+Bx_9)+ax_5-B_0x_7 \\ D^{\alpha}x_8 = \left(\frac{e_0}{N_0}\right)x_6(x_3+Bx_8)-(d+B_0)x_8 \\ D^{\alpha}x_9 = \left(\frac{e_0}{N_0}\right)x_7(x_2+Bx_9)-(d+B_0)x_9 \\ D^{\alpha}x_{10} = d(x_8+x_9)-B_0x_{10} \end{cases}$ (10)	0.96	a = 2, B = 0.9, B_0 = 1/65, d = 52, e_0 = 104, N_0 = 100	x_1 represents susceptibility to all the strains in general, $x_2$and x_3 indicate infections from two different strains, respectively, x_4 and x_5 represent recovery from first and second strain, x_6 and x_7 designate susceptibility to first and second strain, x_8 denotes the infected from the first and cross immunity from the second, x_9 denotes the infected from the second and cross immunity from the first and x_{10} is recovery from both strains.
5.	Fractional-order Migraine (FOM)	$\begin{cases} D^{\alpha}x_1 = \left\{(\epsilon+x_1)0.1+(-x_2-7x_3)\frac{(\epsilon+x_1)^4}{(\epsilon+x_1)^4+1}\right\}(1-x_1)-0.1x_1 \\ D^{\alpha}x_2 = \left\{(1+x_2)0.1+x_1\frac{(1+x_1)^4}{(1+x_1)^4+1}\right\}(1-x_2)-0.1x_2 \\ D^{\alpha}x_3 = \left\{(1+x_3)0.1+23x_1\frac{(\epsilon+x_1)^4}{(\epsilon+x_1)^4+1}\right\}(1-x_3)-0.1x_3 \end{cases}$ (11)	0.87	$1.403 < \epsilon < 1.428$	x_1, x_2 and x_3 represent the respective activities of a population of neighbouring neurons for Trigeminovascular unit, descending modulatory brainstem and cortex unit.

Sl. no.	Disease	Model	a	Parameters	Denotations
6.	Fractional-order Parkinson's illness (FOPI)	$\begin{cases} D^{\alpha}x_1 = G_1 + 1.55x_1 + 6.20x_2 - 7.05x_3 + 0.016x_1^2 + 0.17x_2^2 \\ \qquad - 0.16x_3^2 - 0.1x_1x_2 + 0.13x_1x_3 - 0.082x_2x_3 \\ D^{\alpha}x_2 = G_2 - 2.6x_1 + 2.12x_2 - 2.62x_3 - 0.01x_1^2 + 0.034x_2^2 \\ \qquad - 0.13x_3^2 - 0.17x_1x_2 + 0.32x_1x_3 + 0.025x_2x_3 \\ D^{\alpha}x_3 = G_3 + 1.36x_1 + 3.2x_2 - 3.56x_3 + 0.03x_1^2 + 0.06x_2^2 \\ \qquad - 0.14x_3^2 - 0.14x_1x_2 + 0.09x_1x_3 + 0.08x_2x_3 \end{cases}$ (12)	0.99	$G_1 = -20.93$ $G_2 = 3.87$ $G_3 = -12.12$	x_1, x_2, and x_3 denote points C_3, C_4 and T_5 of the cerebral cortex, central and temporal lobe, respectively.

Table 3:

Analysis of the proposed FO models in their diseased phase

Sl. no.	Disease	Initial Conditions	Equilibrium Points	Eigen Values (λ_i, i = 1,2,3, …, n)	Lyapunov Exponents	Dynamics
1.	FOEVD	(1, 1, 100, 5000)	E_1 = (99.403, 0, 0, 0)	$\lambda_{1,2,3,4}$=(−3.533, −10.82, 5.764 ± 67.012i)	LE_1 = 2.5099, LE_2 = 0, LE_3 = −1.8961, LE_4 = −30.0139	Chaotic
			E_2 = (0.325, 0, 0, 0)	$\lambda_{1,2,3,4}$=(15.995, −14.095, 0.93637 ± 14.85i)		
			E_3 = (51.882, 36.029, 0, 0)	$\lambda_{1,2,3,4}$=(43.31, −6.73, −0.98 ± 55.36i)		
			E_4 = (−0.918, − 0.637, 0, 0)	$\lambda_{1,2,3,4}$=(0.6702, −70.99, 35.475 ± 61.47i)		
2.	FODM	(0.53, 1.31, 1.03)	E_1 = (0.805, 1.815,1.319)	$\lambda_{1,2,3}$= (−1.7563 ± 7.5090i, 1.3802)	LE_1 = 0.39334, LE_2 = 0, LE_3 = −3.7405	Chaotic
			E_2 = (0.624,0.935, 0.877)	$\lambda_{1,2,3}$=(−2.8372, 0.5262 ± 2.3472i)		
			E_3 = (−3.136,2.204,0.724)	$\lambda_{1,2,3}$= (−1.281 ± 11.1566i, 1.1620)		
			E_4 = (0.619, −0.366, 0.864)	$\lambda_{1,2,3}$= (−1.8907 ± 3.7087i, 2.4532)		
			E_5 = (−0.898,1.995,1.119)	$\lambda_{1,2,3}$= (−7.7185, 3.5633, 2.3344)		
3.	FOHIV	(0.06, 0.1, 0.05)	E_1 = (48.6486, 40.8140, 0)	$\lambda_{1,2,3}$=(−0.0706 ± 0.1963i, 0.3381)	LE_1 = 0.020203, LE_2 = 0, LE_3 = −0.017359	Chaotic
			E_2 = (−44.6577, −6.6112, −0.3417)	$\lambda_{1,2,3}$=(0.0321 ± 0.3295i, −0.0161)		
			E_3 = (− 341.47,0,0)	$\lambda_{1,2,3}$= (0.0366, 1.1731, −0.071)		
			E_4 = (1372.7,0,0)	$\lambda_{1,2,3}$=(−0.0366, 0.5908, −0.07)		
4.	FOD	(35.8207, 0.0001, 0.0074, 0.0196, 0.0768, 19.0634, 14.3108, 0.0040, 0, 30.6972)	E_1 = (100, 0, 0, 0, 0, 0, 0, 0, 0, 0)	$\lambda_{1,2,3,4,5,6,7,8,9,10}$=(−0.0154, −0.0154, −2.0154, 51.9846, −0.0154, −2.0154, 51.9846, −0.0154, −52.0154, −52.0154)	LE_1 = 0.051149, LE_2 = 0.034485, LE_3 = 0, LE_4 = −0.025989, LE_5 = −0.049347, LE_6 = −0.12601, LE_7 = −1.8845, LE_8 = −2.1535, LE_9 = −37.4014, LE_{10} = −26.987	Hyperchaotic
			E_2 = (50.1, 0, 0.05, 0, 0.38, 0,49.59, 0, 0, 0)	$\lambda_{1,2,3,4,5,6,7,8,9,10}$=(−0.1540, −2.0150,−0.0154, −52.1540, 2.0150, −0.0310, 0.0298±0.8820 i, −52.0113,46.5019)		
			E_3 = (50.1, 0.015, 0, 0.38,0, 40, 0, 0, 0)	$\lambda_{1,2,3,4,5,6,7,8,9,10}$=(−0.0154, −2.0150, −0.0154, 0.0298 ± 0.8995 i, −2.0150, −0.1696,−52.0154, 52.0140,46.5045)		
			E_4 = −1334.94, 0.21, 0.21, 5.47, 5.47, 1538.84,1538. −0.24, −2.44, −1653.63)	λ1,2,3,4,5,6,7,8,9,10= (0, −1.4133 ± 1.4128i, −1.4652 ± 1.4138 i,−0.0043, 0.0019, 0, −0.0020, −0.0020)		
			E_5 = (34.9, 0.0096, 0.0096, 00.248, 16.715,16.715, 0.0046, 0.0046, 31.073)	$\lambda_{1,2,3,4,5,6,7,8,9,10}$=(−0.0154, −52.0150, −2.2094, −1.7932, −0.1266 ±0.9356 i, 0.082 ±0.78 i, −0.0423)		

Sl. no.	Disease	Initial Conditions	Equilibrium Points	Eigen Values (λ_i, i = 1,2,3, …, n)	Lyapunov Exponents	Dynamics
5.	FOM	(0, −5, −4)	E_1 = (−0.0099, 0.6027, −0.0607)	$\lambda_{1,2,3}$=(−0.1607 ± 7.7796i, −0.2132)	LE_1 = −0.16122, LE_2 = −0.17083, LE_3 = −0.37125	Non-chaotic (stable)
			E_2 = (−1.5592, −0.5136, −0.7935)	$\lambda_{1,2,3}$=(0, −2.1338, −0.8888)		
			E_3 = (1.0137, 0.9191, 0.9955)	$\lambda_{1,2,3}$=(7.3294, −22.2186, −1.2171)		
			E_4 = (0.9887, −1.2559, −1.0674)	$\lambda_{1,2,3}$=(−8.8111, −0.0013, 0.0554)		
			E_5 = (0.9888, −1.2552, −1.0848)	$\lambda_{1,2,3}$=(−8.9288, 0, −0.0001)		
			E_6 = (−1.5532, −1.3483, −0.7933)	$\lambda_{1,2,3}$=(−2.1309, 0, 0.7909)		
			E_7 = (0.9853, 0.9173, −1.0849)	$\lambda_{1,2,3}$=(−6.8178, −1.1902, 0)		
			E_8 = (−0.0056, −1.6101, 0.2554)	$\lambda_{1,2,3}$=(0.2316, −0.100 ± 8.3079i,)		
			E_9 = (1.0191, −1.2523, 0.9955)	$\lambda_{1,2,3}$=(0.2316, −0.1001 ± 8.3079i)		
			E_{10} = (−1.5427, −0.5121, −1.1787)	$\lambda_{1,2,3}$=(0, 1.9314, −0.8853)		
6.	FOPI	(15, 0, 4)	E_1 = (− 187.53, −48.08, −23.30)	$\lambda_{1,2,3}$= (−3.905, 6.81 ±23.94 i)	LE_1 = 0, LE_2 = −0.01, LE_3 = −0.0064675	Non-chaotic (periodic)
			E_2 = (− 3.80, −37.91, −14.8)	$\lambda_{1,2,3}$= (4.96,− 2.31 ± 1.04 i)		
			E_3 = (3.16, 4.62, 2.04)	$\lambda_{1,2,3}$= (0.153,−0.114 ±5.17 i)		

Table 4:

Proposed controllers to stabilise chaos in the biological models of diseases

Disease	Control technique	Parameter values	Controller
FOEVD	BSC	$A_4 = -\left(\frac{b_2}{b_1}\right)x_2$	$u_4 = -b_6(x_4 - A_4)^2 - \left(\frac{b_2}{b_1}\right)x_3 + b_8 x_3^2 - b_4(x_4 - A_4)$
	SMC	$c = 20$, $s = 20$, $L = 10$, $\kappa = 10$	$u_4 = -cx_4 - sign(s)\left(L + \frac{\kappa}{\sqrt{2}}\right)$
	AFC	$w_0 = 1$, $q_1 = 7.01$, $q_2 = 2.894896 \times 10^{-5}$, $q_3 = 0.4135051035$, $q_4 = 0.0184068813$, $q_5 = 5741.076327$, $q_6 = 1.6511395 \times 10^{-5}$, $q_7 = 0.0385601599$, $q_8 = 0.012704823$, $q_9 = -0.47052507$, $q_{10} = -950.142579$, $q_{11} = -0.5516088061$, $q_{12} = -14.91575291$, $q_{13} = -99.6144182$, $q_{14} = 9.1636118$	$u_1 = -w_0x_1 - ((b_1 - q_2)x_2x_4 + (b_2 - q_3)x_2^2 - (b_3 - q_4)x_1x_2)$, $u_2 = -w_0x_2 - w_0x_3$, $u_3 = -w_0x_3 - w_0x_4$, $u_4 = b_{13}x_1 - b_9x_2 + b_7x_3 - q_1x_4 - ((b_4 - q_5) + (b_6 - q_6)x_4^2 + (b_8 - q_7)x_3^2 + (b_{10} - q_8)x_2x_4 + (b_{11} - q_9)x_2x_3 + (b_{12} - q_{10})x_2^2 + (b_{14} - q_{11})x_1 + (b_{15} - q_{12})x_1x_3 + (b_{16} - q_{13})x_1x_2 + (b_{17} - q_{14})x_1^2)$
FODM	BSC	$H_0 = 1$	$u_2 = -H_0x_2 - w_3x_1x_2^2 - w_2x_1^2x_2 + w_1x_1^2 - w_5x_1x_3 + (w_{12} - w_{21})x_3$
	SMC	$c_1 = 11$, $c_2 = 11$, $c_3 = 11$, $s = 8$, $L = 6$, $\kappa = 5$	$u_3 = -c_3x_3 - c_2x_2 - c_1 - sign(s)\left(L + \frac{\kappa}{\sqrt{2}}\right)$
	AFC	$n_1 = 1.35$, $n_2 = 0.03$, $n_3 = 2$, $n_4 = 1.37$, $n_5 = 0.3$, $n_6 = 4.42$, $n_7 = 0.098$, $n_8 = 6.99$, $n_9 = 1.92$, $n_{10} = 1.01$, $n_{11} = 1.41$, $n12 = -0.14$, $n_{13} = 0.8$, $n_{14} = 0.17$, $n_{15} = -0.08$, $n_{16} = -0.66$, $n_{17} = 0.71$, $n_{18} = 1.3$, $n_{19} = -0.04$	$u_1 = -n_1x_1 - n_2x_3 - ((w_2 - n_7)x_1x_2 + (w_3 - n_8)x_2^2 + (w_4 - n_9)x_2^3 + (w_6 - n_{10})x_3^2 + w^7x_3^3 + (w_{20} - n_{11}))$, $u_2 = -n_3x_2 - n_4x_3 - ((w_8 - n_{12})x_1x_2 + w_9x_1^2 + w_{10}x_1^3 + (w_{11} - n_{13})x_2^2 + (w_{13} - n_{14})x_3^2 + (w_{14} - n_{15})x_3^3 + (w_{21} - n_{16}))$, $u_3 = -n_5x_2 - n_6x_3 - ((ww_{16} - n_{17})x_2^2 + (w_{17} - n_{18})x_2^3 + (w_{19} - n_{19})x_2x_3)$
FOHIV	BSC	$H_1 = 1$	$u_2 = -H_1x_2$
	SMC	$c = 4$, $s = 3$, $L = 2$, $\kappa = 2$	$u_2 = -cx_2 - sign(s)\left(L + \frac{\kappa}{\sqrt{2}}\right)$
	AFC	$g_0 = 1$, $S = 1270$, $\frac{R}{K} = -8.13 \times 10^{-5}$, $\frac{\widetilde{\delta\beta_0 d_3}}{\gamma_0} = 0.054$, $P = 4$, $Q = 0.91$	$u_1 = -g_0x_1 - \left((s_0 - S) + \left(\frac{r}{k} - \frac{R}{K}\right)x_1^2 + \left(\frac{\delta\beta_0 d_3}{\gamma_0} - \frac{\widetilde{\delta\beta_0 d_3}}{\gamma_0}\right)\frac{x_1x_2}{(d_1 + x_1)}\right)$, $u_2 = (p_0 - P)x_2x_3 - \frac{\delta\beta_0 d_3 x_1 x_2}{\gamma_0(d_1 + x_1)}$, $u_3 = (q_0 - Q)\frac{x_2x_3}{\varepsilon x_3 + 1}$
FOD	BSC	$H_2 = 1$, $H_3 = 1$, $H_4 = 1$	$u_4 = -H_2x_4 - dx_2$, $u_9 = -H_3x_{10} - d(x_8 + x_9)$, $u_{10} = -H_4x_9 - \left(\frac{e_0}{N_0}\right)x_7x_2$
	SMC	$c_1 = 6$, $s_1 = 4$ $L_1 = 4$, $\kappa_1 = -4$	$u_1 = -c_1x_1 - sign(s_1)\left(L_1 + \frac{\kappa_1}{\sqrt{2}}\right)$
		$c_2 = 4$, $s_2 = 2$ $L_2 = 3$, $\kappa_2 = -2$	$u_5 = -c_2x_5 - sign(s_2)\left(L_2 + \frac{\kappa_2}{\sqrt{2}}\right)$
		$c_3 = 80$, $s_3 = 30$ $L_3 = 20$, $\kappa_3 = -20$	$u_6 = -c_3x_6 - sign(s_3)\left(L_3 + \frac{\kappa_3}{\sqrt{2}}\right)$
		$c_4 = 25$, $s_4 = 2$ $L_4 = 20$, $\kappa_4 = -20$	$u_7 = -c_4x_7 - sign(s_4)\left(L_4 + \frac{\kappa_4}{\sqrt{2}}\right)$

Disease	Control technique	Parameter values	Controller
		c_5=60, s_5=30 L_5=20, κ_5=−20	$u_{10} = -c_5 x_{10} - sign(s_5)\left(L_5 + \frac{\kappa_5}{\sqrt{2}}\right)$
	AFC	$r_1 = \frac{e_0}{N_0} - \frac{\widetilde{e_0}}{N_1}$, $\frac{\widetilde{e_0}}{N_1} = 0.97$, $r_2 = \frac{e_0}{N_0} - \frac{\widetilde{e_0}}{N_2}$, $\frac{\widetilde{e_0}}{N_1} = -0.97$, $r_3 = (d + B_0) - \left(\widetilde{d + B_0}\right)$, $\left(\widetilde{d + B_0}\right) = -104.0154$, $r_4 = (a + B_0) - \left(\widetilde{a + B_0}\right)$, $\left(\widetilde{a + B_0}\right) = -3.0254$, r_5 = 0.9001, r_6 = 0.0346	$u_1 = -(r_1 x_1(x_2 + (B - r_5)x_9) + r_1 x_1(x_1 + (B - r_5)x_8))$, $u_2 = r_3 x_2 - r_2 x_1(x_2 + (B - r_5)x_9)$, $u_3 = r_3 x_3 - r_2 x_1(x_3 + (B - r_5)x_8)$, $u_4 = r_4 x_4 - dx_2$, $u_5 = r_4 x_5 - dx_3$, $u_6 = (B_0 - r_6)x_6 - ax_4 - (r_1 x_6(x_3 + (B - r_5)x_8))$, $u_7 = (B_0 - r_6)x_7 - ax_5 - (r_1 x_7(x_2 + (B - r_5)x_9))$, $u_8 = r_3 x_8 - r_2 x_6(x_3 + (B - r_5)x_8)$, $u_9 = r_3 x_9 - r_2 x_7(x_2 + (B - r_5)x_1)$, $u_{10} = (B_0 - r_6)x_{10} - dx_9 - dx_8$

Table 5:

Proposed anticontrollers to introduce chaos in the biological models of diseases

Diseases	Anticontrol method	Parameter values	Anticontroller
FOM	LSFAC	$Z_1 = 0$; $Z_2 = 10$; $Z_3 = -10$, $Z_4 = -10$; $Z_5 = 0$; $Z_6 = 10$	$x_{a1} = Z_2x_2 + Z_3x_3$, $u_{a2} = Z_4x_1 + Z_6x_3$
	SSSFAC	$\varphi = -10$, $\omega = 10$	$u_{a2} = \varphi \sin(\omega x_3)$
FOPI	SSSFAC	$\varphi = 8$, $\omega = 4$	$u_{a2} = \varphi \sin(\omega x_3)$
	SMAC	$c = 6$, $s = 6$ $L = 4$, $\kappa = 4$	$u_{a2} = -cx_1 - sign(s)\left(L + \frac{\kappa}{\sqrt{2}}\right)$

Table 6:

Comparative analysis of the designed controllers to suppress chaos

Diseases	Controller	Settling Time (t_s) sec	State	MLE	Observation	Physical significance of control action
FOEVD	BSC	20	1	−0.1372	The disease model converges to its equilibrium point E_1 asymptotically (Fig: 3 (a)).	The epidemic of EVD is modelled based on observational data. As a result, the model parameters are empirical. Variation of the tuning parameter þ leads to chaos in the disease model. Prevalence of chaos in the model underlines its tremendous SICs and unpredictability. Any undetected case will result in exponential rise in the number of infections. The controllers designed stabilise chaos in the model and will lead to a timely warning, which is a promising way to stop the epidemic.
	SMC	2.32	1	−2.9213	The disease model converges to E_3 asymptotically (Fig: 3 (b)).	
	AFC	12	4	−0.9873	The disease model converges to E_1 asymptotically. (Fig: 3 (c)).	
FODM	BSC	10	1	−0.7441	The disease model converges to E_2 asymptotically (Fig: 4 (a)).	The fall in population density of β–cells in the pancreas causes Type 1 Diabetes. Parameter w_{15} corresponds to the rate of increase in the population density of β–cells. The increase in glucose level in blood causes Type 2 Diabetes. Parameter w_8 denotes the effect of secreted insulin on glucose level. Excessive secretion of insulin from β–cells causes Hyperinsulinemia. The parameter w_7 denotes the rate of secretion of insulin. Oversecretion of insulin in blood causes Hypoglycemia. Parameter w_1 denotes the reduction of insulin in the absence of glucose. Chaotic behaviour using the above parameters increases unpredictability and is therefore undesirable. The proposed controllers effectively control the model to its stable (non-chaotic) region.
	SMC	11.67	1	−2.5241	The disease model converges to E_3 (Fig: 4 (b)).	
	AFC	5	3	−2.4423	The disease model converges toE_4 asymptotically (Fig: 4 (c)).	
FOHIV	BSC	186	1	−0.0258	The disease model converges to equilibrium point E_4 asymptotically (Fig: 5 (a)).	The pathogen HIV attacks $CD4^+$T cells of human immune system. Excessive low count of $CD4^+$T cells causes AIDS. Parameter d_3 denotes the virus replication factor and is one of the control parameters. For certain values, chaos may result that may enhance the death rate of $CD4^+$T cells and thus the disease progression. The controllers are designed so as to direct the system to stable dynamics rather than chaos.
	SMC	182	1	−0.0266	The disease model converges to E_4 (Fig: 5 (b)).	
	AFC	10	3	−0.1621	The disease model converges to its equilibrium point E_4 asymptotically (Fig: 5 (c)).	
FOD	BSC	110	3	−0.0440	The disease model converges to equilibrium point E_2 asymptotically (Fig: 6 (a)).	For the two coexisting strains of Dengue fever considered in the model, the measure of infectiousness, B, is responsible for chaotic dynamics. The controllers counter the effects of this parameter to stabilise chaos.
	SMC	2	5	−2.0533	The disease model converges to origin asymptotically (Fig: 6 (b)).	
	AFC	109	10	−0.0140	The disease model converges to E_1 asymptotically (Fig: 6 (c)).	

Table 7:

Comparative analysis of the designed anticontrollers to induce chaos

Disease	Anticontrol	State	MLE	Observation	Physical significance of anticontrol action
FOM	LSFAC	2	2.3888	Initially stable trajectories turn chaotic after addition of controller at 100s. (Fig. 7 (a))	Parameter ϵ denotes the basal excitability of the neuron networks. The value of ϵ for which the model displays stable dynamics causes the prodromal phase of Migraine without aura. On introducing the designed anticontrollers to this diseased phase, it is found that chaos is generated to ensure complex excitation of neurons. Thus, they are effective since a healthy brain normally is chaotic.
	SSSFAC	1	0.9737	Initially stable trajectories turn chaotic after addition of controller at 100s. (Fig. 7 (b))	
FOPI	SMAC	1	0.20504	Initially periodic trajectories turn chaotic after addition of controller at 100s (Fig. 8 (a))	The EEG signals extracted from the central and temporal lobes of the cerebral cortex display periodic or stable dynamics on the onset of FOPI that destroys the normal process of the brain. The positive MLEs show that the anticontrollers designed lead to generation of chaos in the brain signals to bring them to normal healthy functioning.
	SSSFAC	1	0.25712	Initially periodic trajectories turn chaotic after addition of controller at 100s. (Fig. 8 (b))	